INSTITUT DE FRANCE
Académie des sciences

Comptes Rendus

Chimie

Nabila Aprianti, Muhammad Faizal, Muhammad Said and Subriyer Nasir

H_2-rich syngas production by sorption enhanced steam gasification of palm empty fruit bunch

Volume 25, Special Issue S2 (2022), p. 155-167

Published online: 6 July 2022

https://doi.org/10.5802/crchim.192

Part of Special Issue: Sustainable Biomass Resources for Environmental, Agronomic, Biomaterials and Energy Applications 3

Guest editors: Mejdi Jeguirim (Université de Haute-Alsace, Institut de Sciences des Matériaux de Mulhouse, France), Salah Jellali (Sultan Qaboos University, Oman) and Besma Khiari (Centre of Water Researches and Technologies, Tunisia)

Les Comptes Rendus. Chimie *sont membres du*
Centre Mersenne pour l'édition scientifique ouverte
www.centre-mersenne.org
e-ISSN : 1878-1543

Comptes Rendus
Chimie
2022, Vol. 25, Special Issue S2, p. 155-167
https://doi.org/10.5802/crchim.192

Sustainable Biomass Resources for Environmental, Agronomic, Biomaterials and Energy Applications 3 / *Ressources de biomasse durables pour des applications environnementales, agronomiques, de biomatériaux et énergétiques 3*

H_2-rich syngas production by sorption enhanced steam gasification of palm empty fruit bunch

Nabila Aprianti [a, b], **Muhammad Faizal** [*, b], **Muhammad Said** [b] **and Subriyer Nasir** [b]

[a] Doctoral Program of Environmental Science, Graduate School, Universitas Sriwijaya, Palembang 30139, South Sumatra, Indonesia

[b] Chemical Engineering Department, Faculty of Engineering, Universitas Sriwijaya, Ogan Ilir 30662, South Sumatra, Indonesia

E-mails: nabilaaprianti5@gmail.com (N. Aprianti), muhammadfaizal@unsri.ac.id (M. Faizal), m.said@unsri.ac.id (M. Said), subriyer@unsri.ac.id (S. Nasir)

Abstract. Hydrogen-rich syngas from palm empty fruit bunch has been produced using CaO and bentonite as absorbent and catalyst. The gasification process is carried out at 550–750 °C at atmospheric pressure in the fixed bed gasifier with steam to biomass ratio (S/B) of 0–2.5 and Ca/C ratio of 0–2. The results showed that CaO only acts as CO_2 absorbent during the process. Increasing the ratio of Ca/C and S/B has increased the concentration of H_2 and absorption of CO_2 in the syngas. The addition of CaO did not significantly increase the production of CH_4 and CO in the syngas. The H_2 concentration reaches about 78.16 vol% at 700 °C and Ca/C 2.

Keywords. H_2 purity, Palm waste, Steam gasification, Catalytic gasification, CO_2 absorption.
Published online: 6 July 2022

1. Introduction

Global warming is a serious environmental problem that threatens the survival of all living beings. Global warming is mainly caused by the accumulation of carbon dioxide in the atmosphere. CO_2 is responsible for at least 76% of all greenhouse gas (GHG) emissions, with 65% arising from fossil fuel combustion and industrial usage [1–3]. In addition, fossil energy reserves continue to decline, accompanied by rising crude oil prices. The use of renewable energy to substitute fossil fuels is one way to reduce CO_2 emissions. As the prime renewable carbon source with neutral carbon, biomass is an alternative energy source that can be utilized side by side with fossil fuels.

Biomass is a renewable energy source that is compatible with fossil energy. Knowledge in developing biomass conversion technology and filling gaps needs to be deepened. Agricultural and plantation waste that is not competitive in the food sector is a suitable energy source. Being the largest palm oil exporter, Indonesia produced and exported nearly 45 million tons of palm oil and 26 million tons in 2020. For every ton of crude palm oil produced, there are around 1.5–2 tons of palm empty fruit bunch

* Corresponding author.

(PEFB), or 22% of the whole process [4–7]. PEFB is a by-product of sterilizing and stripping oil palm fruit from fresh fruit bunches [8,9]. PEFB is occasionally allowed to decompose on the discharge side, creating anaerobic conditions with strong greenhouse gas (GHG) emissions of methane [10]. The current practice of PEFB disposal is by burning to produce steam to generate electricity in palm oil mills [11] or used as organic fertilizer [12]. Direct combustion of PEFB as biomass has several disadvantages: low calorific value, high moisture content, corrosion problems, wide particle size distribution, and low homogeneity [13–15]. However, since PEFB mainly comprises cellulose, hemicellulose, and lignin, processing wastes such as anaerobic digestion without pre-treatment will be complex [13,16,17].

To improve the properties of biomass fuels, many conversion processes have been applied to obtain high-quality fuels from biomasses. Biomass conversion can be carried out by various processes such as thermochemical, bioprocesses, and various physical and chemical processes [18–20]. Gasification as thermochemical conversion technology can effectively convert biomass into syngas consisting of H_2 and CO. Utilization of biomass becomes real and valuable through gasification, which produces high purity H_2. However, there are still limitations in increasing the added value of biomass. Carbonaceous gases such as CO, CH_4, and CO_2 are also present in the syngas, which dilutes the H_2 concentration. Sorption enhanced steam gasification (SESG) is a simple and novel technology to produce H_2 rich syngas from biomass. CaO is used as an absorbent in the process to remove CO_2, which is formed directly during the gasification process. This increases the concentration of H_2 in the syngas. The optimal temperature based on literature studies is 500–750 °C under atmospheric pressure [21–25]. This is related to CO_2 absorption so that syngas rich in H_2 and low in CO_2 concentration is obtained.

Research on SESG using CaO has been carried out on several biomasses. Martinez *et al.* [26] used wood and wheat straw as feedstock in the steam gasification process with absorption focused on tar formation. Inayat *et al.* [27] obtained 75 vol% H_2 from EFB at 700 °C. In addition to the steam ratio, temperature also affects the gasification process by absorption. At 750 °C, CaO only acts as the catalyst to increase the carbon conversion rate. The maximum CO_2 absorbed by CaO was 189.88 mL/g in the gasification of cellulose by Mbeugang *et al.* [28]. Sufficiently high H_2 concentrations were also obtained for sugarcane leaves by the same process using CaO/MgO at 600 °C [29]. Dong *et al.* [30] also confirmed that the addition of CaO to biochar increased H_2 at 700 °C. Detchusananard *et al.* [31] stated that the ratio of S/C and gasification temperature were the parameters that most influenced the gasification of wood residue. However, the carbon conversion and gasification efficiency of the SESG process are pretty low at the existing gasification temperature range. Gasification of biomass at lower temperatures will produce high tar. Although CaO has been shown to catalyze cracking or reformation, tar is still formed during the gasification process. There are two main ways to increase H_2 yield further and reduce tar from the current SESG process. One method adds pressure to the process to raise the reaction temperature [32–34]. Under pressure, a higher gasification temperature can be achieved to increase the CO_2 absorption rate. Meanwhile, in such a case, the gasification efficiency and the conversion rate of biomass carbon will be greatly improved, significantly increasing the yield of high-purity H_2. The key problems in this method are the pressurized system's great complexity and difficulty of the operation and the high capital and operational expenditure. Another option is to include a catalyst in the process to speed up the gasification reaction [27,35,36].

Bentonite has been widely used as an absorbent and catalyst in several waste treatment processes [37–40] and energy conversion, especially pyrolysis [41–45]. In our previous study [46,47], the application of bentonite was shown to increase H_2 in conventional gasification at low temperatures. In addition, bentonite can reduce tar during the gasification process [48] and increase the heating value of the gas as an adsorbent [49]. To the best of our knowledge, there is very limited literature discussing catalytic sorption enhanced steam gasification of PEFB to obtain high H_2 concentrations in syngas. Moreover, a bentonite catalyst has never been applied to this process. This study aims to produce H_2-rich syngas from PEFB through the SESG catalytic process. Parameters evaluated were the effect of temperature, steam to biomass ratio, and Ca/C ratio on syngas composition, H_2 increase, and CO_2 reduction, as well as calorific value and gasification

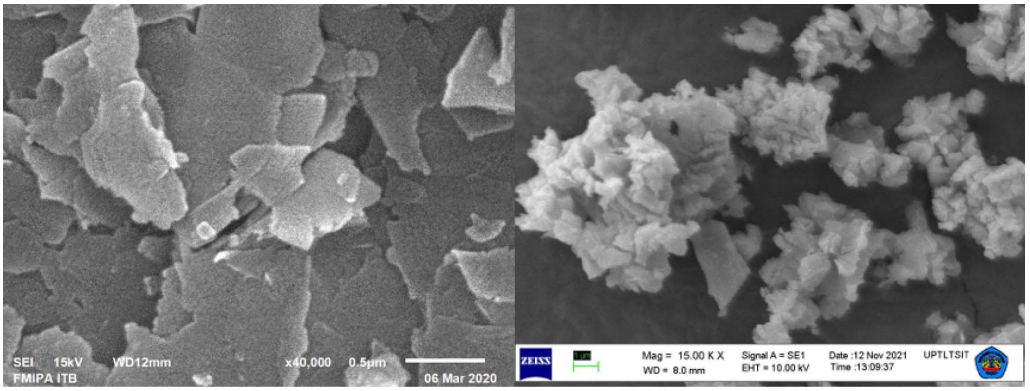

Figure 1. SEM image of (a) bentonite and (b) CaO.

efficiency.

2. Materials and methods

2.1. *Feedstock*

Palm empty fruit bunch in this study was obtained from the local crude palm oil industry in South Sumatra, Indonesia. The analysis and results of proximate and ultimate PEFB and bentonite as a catalyst in this study were reported in our earlier studies [46,47]. The absorbents used in this study consist of 96.23% CaO, and 1.75% MgO, and the rest are Fe_2O_3, SiO_2, K_2O_3, as well as Al_2O_3, each of which are less than 1% as determined by XRF analysis. The morphology of CaO and bentonite is seen from Scanning Electron Microscope (SEM) images (Figure 1). SEM microscopy was performed using SEM JEOL-JSM-6510 LA. As seen, calcined bentonite has a simple structure while calcined CaO possesses a loose structure, and the active surface is quite porous and rough, which is suitable for CO_2 uptake.

2.2. *Experiments*

The gasification apparatus shown in Figure 2 consists of a gasifier (OD 230 mm and height 670 mm), a cleaning system, a biomass hopper, and a cooling system. The gasifier was made of stainless-steel pipe with a thickness of 15 mm and was heated by three electrical heaters to reach reaction temperature (550–750 °C). The gasification process was carried out in a fixed bed gasifier, with steam serving as the gasification agent and being injected into the bottom of the gasifier. At the beginning of the process, the CaO is placed in the bed that is upper from feedstock and catalyst. The gasification products passed through the cooling system. Tar was separated after cooled and collected in the storage tank. Gas chromatograph (Perkin Elmer Clarus 680) was used to evaluate the syngas composition after being collected in the gas bag. Steam gasification of PEFB with bentonite catalyst was performed at temperatures between 550 °C to 750 °C, and the ratio of steam to biomass (S/B) varied from 0 to 2.5. The Ca/C revealed the CaO and carbon ratio in PEFB varied from 0 to 2.

3. Results and discussion

3.1. *Effect of variation of catalytic gasification temperature on* $S/B = 1$

Syngas yield and syngas composition from palm empty fruit bunch (PEFB) catalytic gasification at different temperatures are shown in Figure 3. Syngas yield increased gradually with increasing temperature. At 750 °C, the syngas yield reached 1.03 m^3/kg. These results indicated the potential of PEFB to produce syngas. This finding aligns with SESG results from other feedstocks, which show that higher temperatures favor carbon conversion, resulting in higher syngas yields [28,50,51].

The concentration of H_2 increased with increasing temperature, while, the opposite trend was found

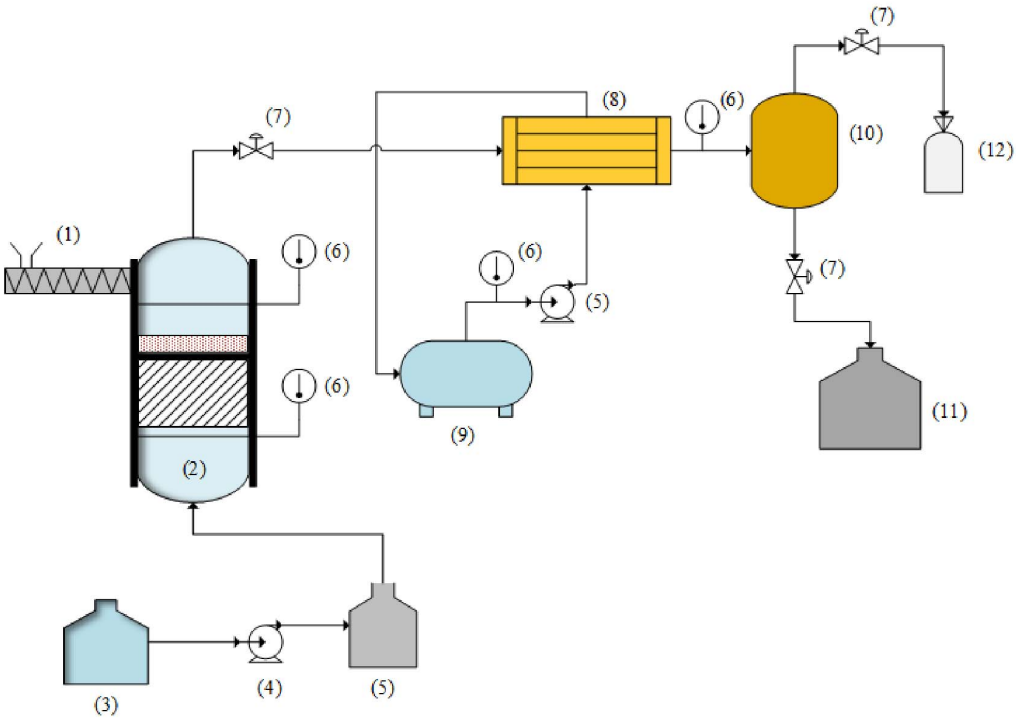

Figure 2. Illustration of the experimental setup for SESG of PEFB. (1) Biomass hopper; (2) gasifier; (3) water tank; (4) pump; (5) steam generator; (6) temperature controller; (7) valve; (8) heat exchanger; (9) cooling water tank; (10) separator; (11) liquid storage; (12) gas bag.

for CO. Kinetically, the increasing temperature is suitable for the water gas shift (WGS) reaction to produce H_2 to a certain extent. Gasification can take place at low temperatures, such as in this study, with a temperature range of 550–750 °C. It is still necessary to support the absorption process and a catalyst to optimize the gasification reaction in PEFB. With increasing temperature, the concentration of H_2 increases rapidly so that the H_2 in the syngas reaches 42.15 vol%. The increase in H_2 is also influenced by the bentonite catalyst used. Our previous work revealed that H_2 increased after bentonite was applied [46]. The concentration of CH_4 is marginally increased due to the breaking of the branching of the volatile molecule. CO was also generated during the cracking and reforming processes, although it was insignificant. If there is a quick increase in H_2 and CH_4 concentrations, the WGS reaction will consume some of the CO, resulting in a continual reduction in CO concentration. The concentration of CO, which was initially high at 40.12 vol%, decreased to 31.24 vol% at 750 °C. With increasing gasification temperature, the concentration of CO_2, which was initially reduced and then increased, obtained a minimum value of 13.26 vol% at a temperature of 650 °C. CO_2 is formed from the primary cracking of the C=O functional group in the PEFB biomass molecule, steam reforming from volatile pyrolysis, and the WGS reaction.

The cracking and reformation of the volatiles are generally sufficient around 650–750 °C. During the PEFB steam gasification process, the WGS reaction rate increases and becomes the dominant reaction. As the temperature rises from 650 to 750 °C, the reaction rate of the WGS reaction increases, causing the CO content to drop progressively and the concentrations of H_2 and CO_2 to rise. In addition, steam reforming of CH_4 occurs significantly at higher temperatures, leading to a decrease in its concentration. According to Figure 3, the concentration of H_2 in the syngas is relatively low (29.65–42.15 vol%) because a substantial amount of carbon gas (CO, CH_4, and CO_2)

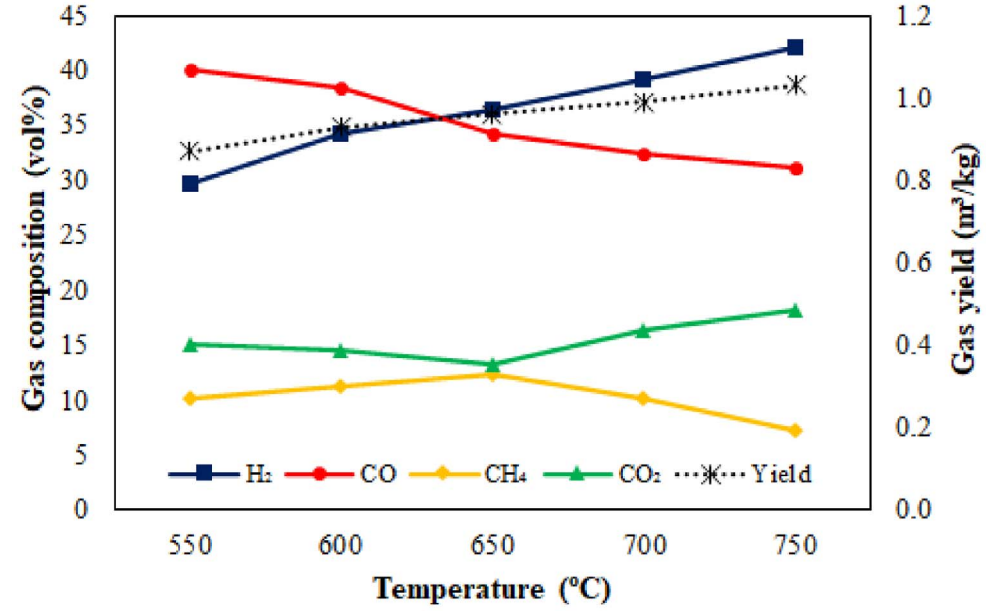

(a)

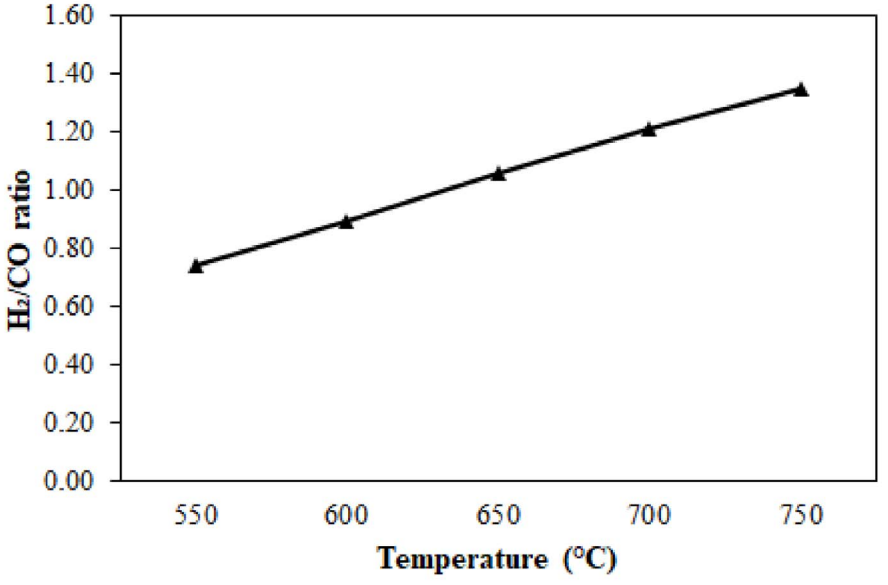

(b)

Figure 3. Effect of gasification temperature on (a) syngas composition and yield, (b) H_2/CO ratio at S/B = 1.

is still present, diluting the H_2 concentration. A major portion of carbon-containing components may be transformed to H_2 by steam reforming and the WGS reaction, and CO_2 can be decreased further from the resulting gas, higher yields of high-purity H_2 are expected. Temperatures above >650 °C do increase H_2, but CO_2 increases 5 vol%. From the PEFB gasification process with S/B = 1, the maximum H_2 was achieved

at 700 °C.

The H_2/CO ratio is a benchmark for classifying the use of advanced fuels. In Figure 3b, the ratio of H_2/CO at various gasification temperatures is presented. At 550 °C and 600 °C, the H_2/CO ratio obtained is relatively low because it is deluded by the high CO content. In this condition, the effect of the catalyst is powerful to produce CO through the Boudouard reaction, water gas reaction, and steam methane reforming. The H_2/CO ratios at 550 °C and 600 °C were 0.74 and 0.89, respectively, suitable for ethanol production [52]. The high CO concentration causes the H_2/CO ratio to be less than two. The syngas produced at this stage is only suitable for producing aldehydes and alcohols. Therefore, improving the quality of H_2 to achieve a higher H_2/CO ratio is carried out at a later stage.

3.2. *Effect of S/B variation on syngas composition from PEFB*

In the previous catalytic steam gasification process, a high concentration of H_2 was produced at 700 °C with S/B = 1. Therefore, gasification was continued by varying the S/B, focusing on increasing H_2. An increase in H_2 volume indicates success in quality improvement. The addition of steam is beneficial for the re-formation of methane (methane reforming reaction). For gasification at atmospheric pressure, as in the present study, more steam is needed to enrich the H_2 content and provide adequate mixing to encourage the reaction to completion. Steam is used to enrich the volume fraction H_2 in the final product. The steam to biomass (S/B) ratio is calculated by dividing the steam flow rate by the biomass mass flow rate on a dry basis.

Figure 4 shows the syngas composition and yield from PEFB steam gasification with variation steam to biomass (S/B). As expected, the steam injection in the process increased in the total syngas yield and volume fraction of H_2. An increase in S/B from 0.5 to 2.5 indicates a gradual increase in gas yield and H_2 concentration from 0.99 m^3/kg to 1.36 m^3/kg and 39.21 vol% to 49.26 vol%. This is due to the rise in S/B ratio increasing the partial pressure of steam in the gasification system, thereby increasing the gasification of volatile steam and char, and the WGS reaction to produce more H_2. However, because the S/B ratio exceeded 1.5, the concentration of H_2 and the ratio of H_2/CO had decreased and increased slowly (Figure 4b). This indicates that additional steam is large enough for the steam gasification process. A significant excess of steam will also increase the system's overall energy consumption. Thereupon, the S/B ratio should not be too high during the gasification process.

The volume of H_2 increased as the S/B ratio increased, while the volume of CO and CH_4 decreased. The addition of steam to the gasification process raises the partial pressure of steam in the gasifier, which aids the reaction of water–gas shift and steam reforming, resulting in increased H_2 generation [53]. The volume of H_2 increased by 13.69% after steam was injected at 550 °C, while the volume of CO decreased by 10.90%. The presence of steam in the gas phase reaction results in the decomposition of hydrocarbons and an increase in the content of H_2 and CO_2 as reaction products. These results are supported by research conducted by Lei and Zhou [54], who found a significant increase in H_2 while CO decreased drastically.

Low heating value (LHV) decreased with an increase in the S/B ratio from 11.94 to 8.61 MJ/N·m^3. The principal contributors to LHV are H_2, CO, and CH_4. The decrease in LHV gas was caused by the reduced content of CH_4 and CO because they have a more significant contribution to LHV gas. This system works well in calorific value, as seen from the slight decrease in calorific content. A reduction in the calorific value of gases for steam gasification was also investigated by Rupesh *et al.* [55]. The decline in calorific value was caused by a decrease in the high energy content of the gas (CH_4 and CO) at an S/B ratio higher than 1. The drop in CO and CH_4 levels was seen to be greater than the rise in H_2 content. The lower calorific value of the biomass and product gas determines the efficiency of the cold gas to evaluate the performance of the gasification system.

Figure 5 depicts the effect of S/B ratio changes on carbon conversion (CCE) and cold gas efficiency (CGE). The carbon conversion and cold gas efficiencies are higher at S/B ratio of 0 and decrease with increasing S/B ratio. The reduction of efficiencies was driven by descending the CH_4, CO, and CO_2 concentrations. Meanwhile, the CGE decreased due to the increase in the S/B ratio from 95.14% to 80.14% because it was related to the LHV gas, which de-

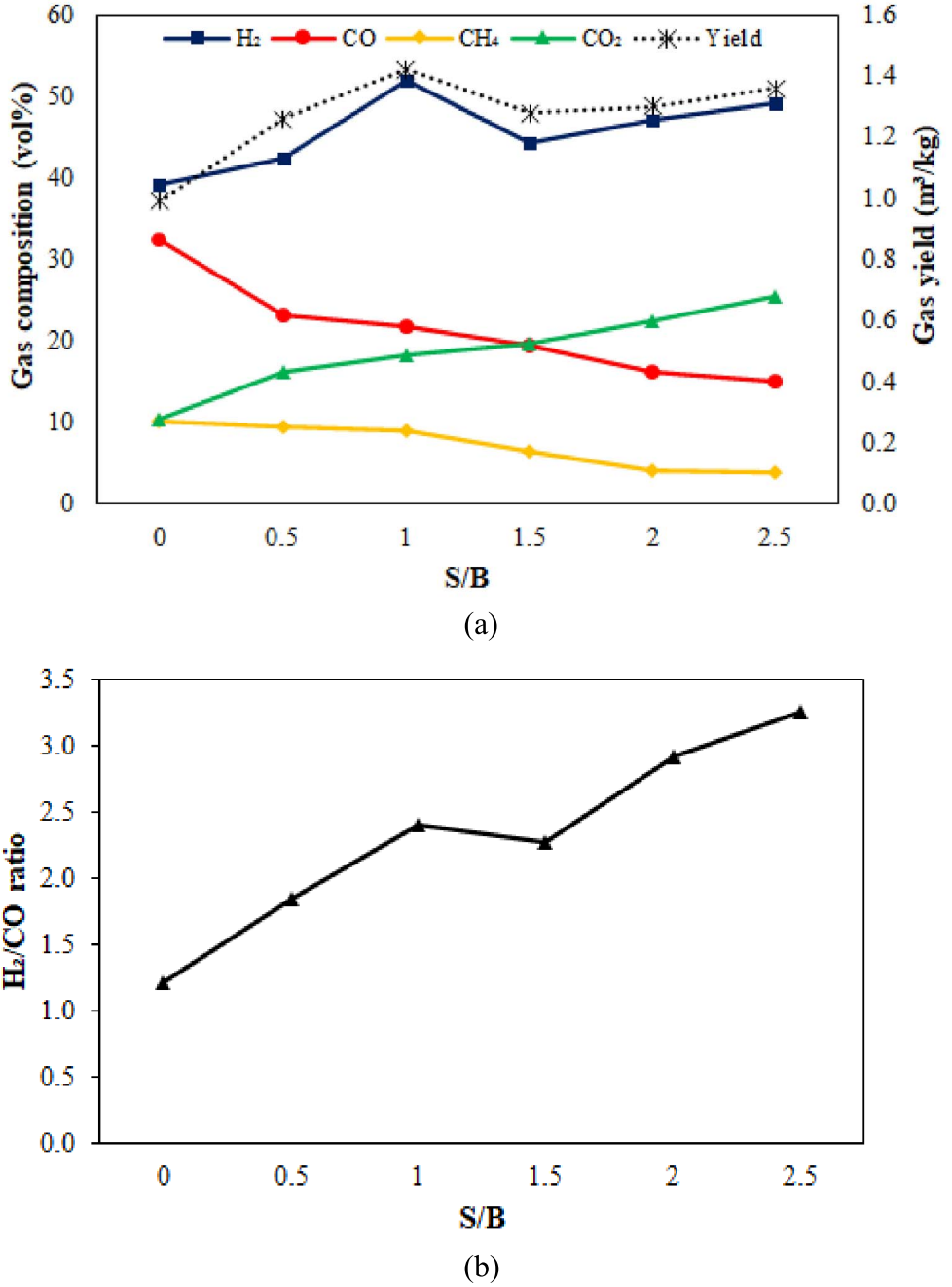

Figure 4. Effect of S/B variation on (a) syngas composition and yield and (b) H_2/CO ratio of PEFB catalytic gasification.

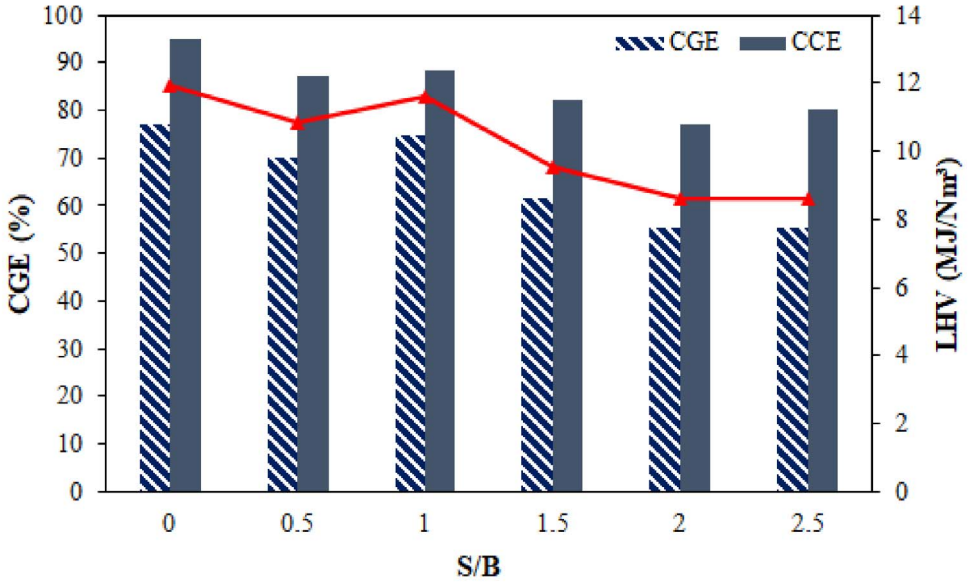

Figure 5. Effect of S/B ratio on cold gas efficiency and LHV syngas.

creased with the increase in the S/B ratio. Shahbaz *et al.* [56] and Tavares *et al.* [57] also reported a similar trend.

3.3. *Effect of variation of CaO/PEFB ratio (wt/wt) on syngas quality*

The PEFB gasification process with absorption was carried out at different variations of CaO. In addition, after the temperature was increased by more than 700 °C on steam gasification, the CO_2 concentration continued to increase, and the WGS reaction was active under these conditions. It prevented the reverse carbonation reaction [58]. Figure 6 shows the syngas composition and yield from PEFB steam gasification with various ratios of CaO/PEFB. The total syngas yield and the concentration of H_2 in syngas increase with increasing the Ca/C ratio. Syngas yield increased from 1.52 m^3/kg to 1.83 m^3/kg, rising Ca/C from 0 to 2. The concentration of H_2 in the produced gas also increased from 52.05 vol% to 68.16 vol%, while decreasing the concentration of CO from 21.57 to 9.15 vol%. The same trend also occurred in the CO_2 concentration, which dropped slightly from 17.26 vol% to 9.64 vol%. The fundamental reason for this is that the in-situ CaO absorbs the CO_2 produced during the gasification process, causing the chemical balance of the WGS reaction to shift with more H_2 being produced. CO_2 absorbed by CaO through the carbonation reaction causes WGS to be more dominant to produce H_2 than the Boudouard reaction because CO_2 as a reactant has been reduced.

The concentration of CH_4 did not show a significant increase with the addition of CaO, which was still maintained at a relatively high concentration. Li *et al.* [59] also stated that steam could activate CaO, thereby increasing the reactivity of CO_2 absorption by CaO and increasing H_2 concentration. S/B variations were not carried out in gasification using CaO because, based on the previous literature, there was a decrease in the partial pressure of CO_2 in the product gas, which reduced the ability of CaO to absorb CO_2. This can weaken the effect of increasing the addition of CaO in the H_2 production process. As for the CH_4 concentration, its contents remained stable, indicating that CaO has little impact on CH_4 reforming under the experimental conditions of this study. The H_2/CO ratio is a quality indicator for syngas. As shown in Figure 6, the H_2/CO ratio increased significantly along with the increase in CaO. The highest increase mainly occurred when the Ca/C was increased from 1.5 to 2. When CaO was not added, the H_2/CO

ratio was only 2.41 but then increased to 7.45 with the maximum addition of CaO. According to Guzman *et al.* [60], syngas with H_2/CO ratio > 2 are suitable for fuel, Fischer–Tropsch synthesis, and methanol.

Figure 7 shows that CO_2 absorption by CaO increased significantly as Ca/C increased from 0.5 to 1 and continued to increase at a consistent pace when Ca/C grew from 1.5 to 2. The percentage of CaO absorbed was 61.53%. Increasing the Ca/C thickens the bed to prolong the residence time of tar vapours and gases such as CO and CO_2 in the absorbent layer. Thus, the cracking reaction of the tar compound on the surface of the CaO particles and the WGS reaction became more intense as more CO_2 was absorbed by the high absorbent, resulting in more CO being transformed into H_2. The increase in H_2 almost doubled after the S/B = 1 and Ca/C = 2 ratios were applied. It becomes a reactive condition of CaO in the carbonation reaction, and an increase in H_2 occurs through the WGS reaction. The synergistic effect of the two materials has a favorable impact on improving the quality of the syngas.

The low heating value decreased from 11.58 to 10.73 MJ/N·m^3 with an increase in the Ca/C ratio from 0 to 2.5 due to a decrease in the content of CH_4, CO, and CO_2, as shown in Figure 8, while a slight increase in LHV gas was observed when the Ca/C ratio was further improved. Carbon conversion and cold gas efficiency decreased to 51.85% and 69.15%, respectively, with a ratio of 2. The carbon conversion efficiency value was lower than the cold gas efficiency because it was measured based on the carbon content in syngas. The same trend has been described in the literature [61].

3.4. *Correlation analysis between the operating condition of PEFB gasification*

Analysis of variance (ANOVA) was used to test the significance level of individual research variables. Table 1 displays the results of the analysis of variance (ANOVA). From the results of ANOVA analysis, it was found that the coefficient of determination (R^2) and the value of determination adjustment (Adj. R^2) were high for Ca/C and temperature, which explained that these two variables significantly affected the gasification process. The p-value < 0.05 has also determined that the variable is significant. Of the three experimental variables, Ca/C was the most significant in increasing the concentration of H_2 with a p-value of 0.00095, followed by temperature with a p-value of 0.00277. Nevertheless, the steam to biomass ratio did not support the production of H_2 because it only has an effect of 12%, and the p-value > 0.05, so it is considered insignificant. It can be concluded that the Ca/C ratio and temperature are the most important parameters in producing H_2-rich syngas in PEFB gasification.

Principal component analysis (PCA) was performed to analyze the correlation between gasification operating variables [62]. Figure 9 shows the direction of the eigenvectors of temperature, S/B, and Ca/C for the syngas composition, where a1–a5 corresponds to the temperature of 550–750 °C, ab1–ab5 corresponds to the S/B ratio of 0.5–2.5, and ac1–ac5 corresponds to Ca/C ratio of 0–2. PCA chart shows the part of each parameter that affects the production of H_2. Almost all research variables except temperature of 550 °C have eigenvectors with the same direction and small angle. They are positively correlated with H_2 concentration, which is also confirmed by the results of the Pareto chart (Figure 10). Meanwhile, the eigenvectors with opposite directions show that the research variables are inversely correlated with CH_4 and CO_2.

The steam gasification process enhanced by absorption using CaO in other studies is presented in Table 2 to compare research results. It is worth noting that, PEFB has also been exploited with a similar process by Inayat *et al.* [27], which uses zeolite as a catalyst. The maximum H_2 concentration produced is 75 vol%. In general, the characteristics of the PEFB used were similar when viewed from the proximate and ultimate analysis, but the concentration of H_2 in this study was higher. Besides PEFB, waste from the CPO industry that has been utilized is palm kernel shell (PKS). Shahbaz *et al.* [36,56] investigated simulated and experimental PKS gasification that obtained high H_2 concentrations for both studies (79.32 and 79.77 vol%). Coal bottom ash is used as a catalyst to increase H_2. The higher H_2 concentration in PKS was influenced by the higher volatile matter and carbon content than PEFB in this study. This is also consistent with other studies using different biomass, which got different H_2 due to different volatile matter and carbon content [23]. In addition, the steam ratio used in this study is higher so that the energy input is more. Comparing the results with

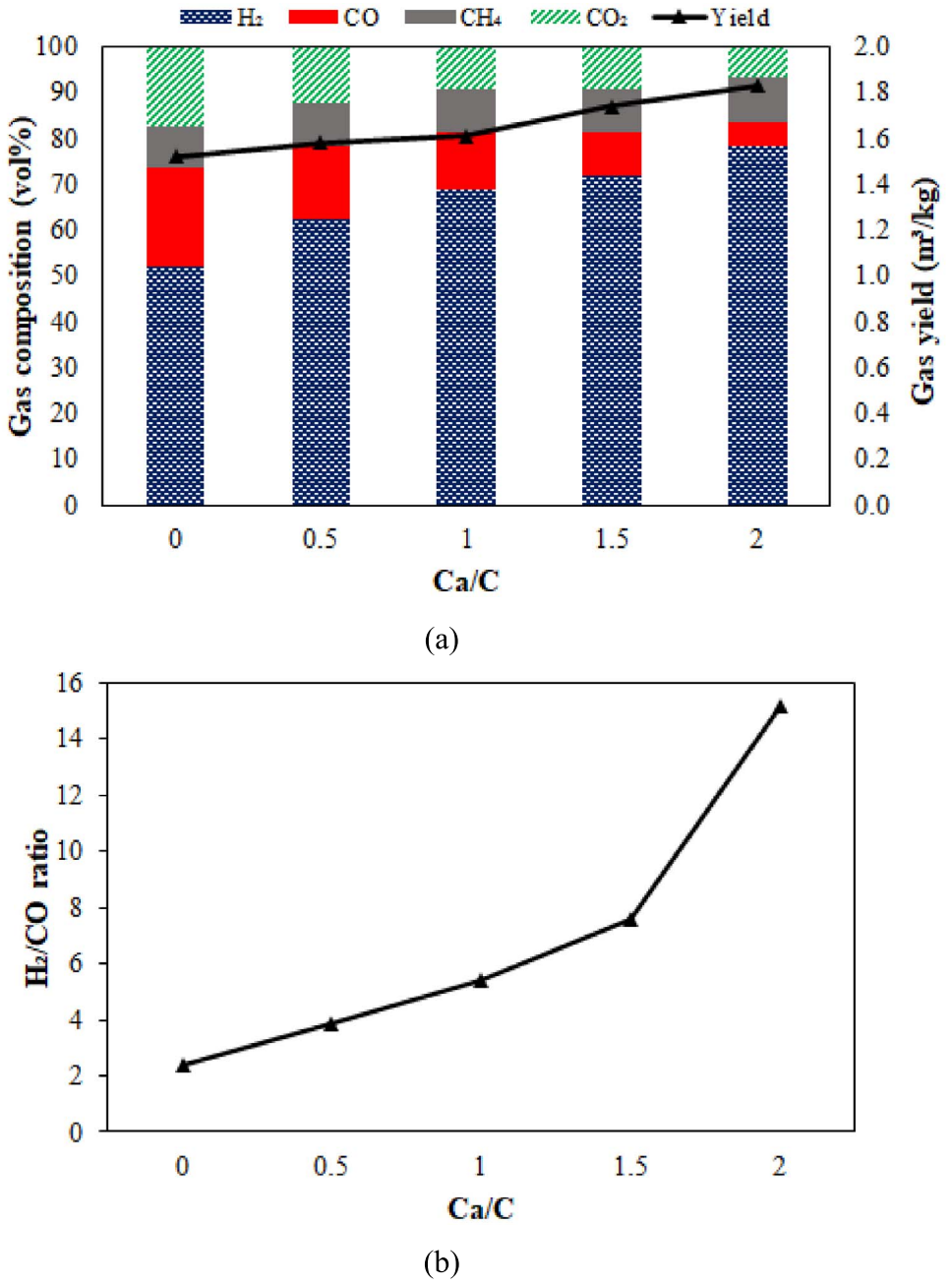

Figure 6. Effect of Ca/C ratio on (a) the syngas composition and yield and (b) H_2/CO ratio of PEFB sorption steam gasification.

published literature shows that the gasification process in this study makes it possible to generate large amounts of hydrogen from PEFB waste and compete.

4. Conclusion

Steam gasification enhanced by absorption in palm empty fruit bunch was carried out in a fixed bed reactor. The effect of gasification temperature, steam to biomass ratio, and Ca/C ratio on hydrogen-rich

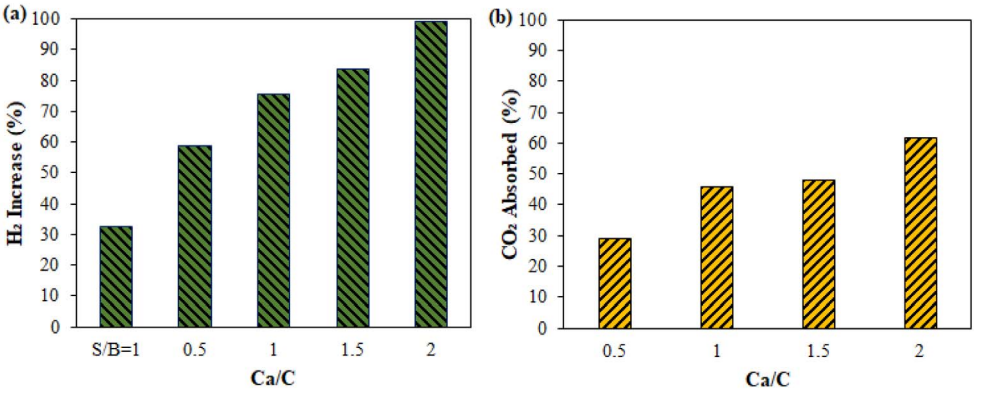

Figure 7. Effect of Ca/C ratio on the percentage increase in H_2 and CO_2 absorption in the catalytic gasification of PEFB.

Table 1. Statistical analysis of parameters affecting H_2 production

Parameter	*F*-value	*P*-value	R^2	Adj. R^2
Temperature (°C)	83.46527	0.00277	0.96530	0.95374
S/B	0.43218	0.55786	0.12592	−0.16544
Ca/C	172.85330	0.00095	0.98294	0.97725

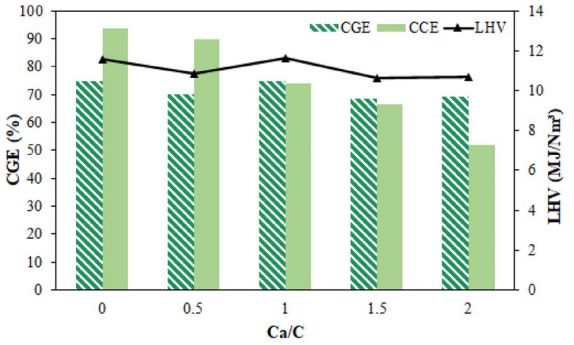

Figure 8. Effect of Ca/C ratio on cold gas efficiency and LHV syngas.

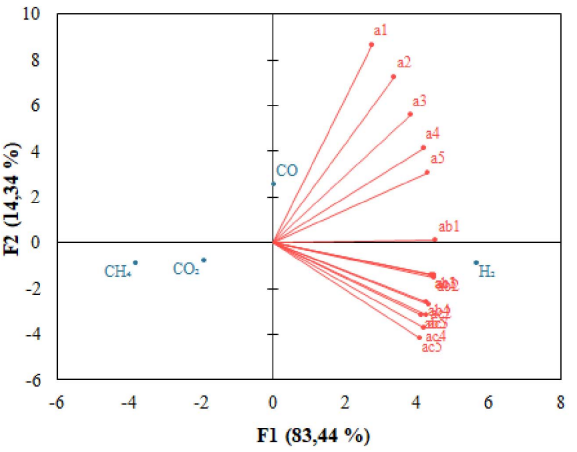

Figure 9. PCA plot of operating variables on syngas composition.

syngas production was investigated. CaO plays the role of an absorbent in the gasification process, characterized by the absorption rate of CO_2 reaching 61.53%. The addition of CaO makes the water gas-shift reaction dominant to produce more hydrogen. At 700 °C, S/B ratio of 1 and Ca/C ratio of 2, the maximum syngas yield and H_2 concentrations obtained were 1.83 m^3/kg and 78.16 vol%, respectively. Based on statistical analyses, the temperature and Ca/C ratio are variables that affect H_2 production significantly. The absorption process in steam gasification of palm empty fruit bunch has succeeded in producing quality syngas rich in hydrogen.

Conflicts of interest

Authors have no conflicts of interest to declare.

Table 2. Summary of syngas production via the sorption enhanced steam gasification of biomass reported in the literature

Feedstock	H_2 (%)	Operation condition	References
PEFB	78.16	T = 700 °C S/B = 1 Ca/C = 2	Present study
PEFB	75	T = 700 °C S/B = 2 Ca/C = 1	[27]
PKS	79.77	T = 692 °C S/B = 1.5 Ca/C = 1.42	[36]
PKS	79.32	T = 700 °C S/B = 1.5 Ca/C = 1.42 Simulation	[56]
Pine sawdust	76	T = 650 °C Ca/C = 2	[63]
Corn stalks Rice straw Wheat Straw Peanut shell	61.23 60.28 58.69 60.84	T = 650 °C S/B = 1 Ca/C = 1	[23]

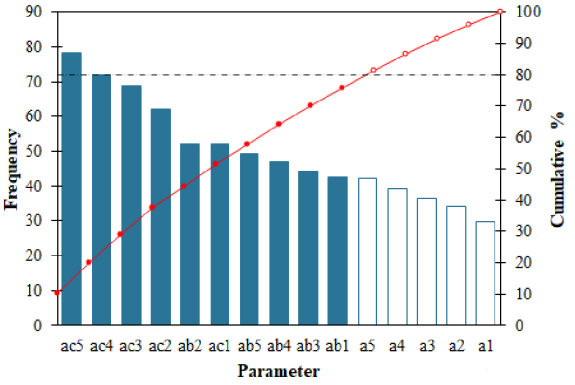

Figure 10. Pareto chart of PEFB gasification parameters for H_2 production.

Acknowledgments

This research was supported by Ministry of Education, Culture, Research, and Technology of the Republic of Indonesia through PMDSU scheme (Grant Number: 054/E4.1/AK/04.PT/2021 and 0163/UN9/SB3.LP2M.PT/2021).

References

[1] I. S. Farouq, N. Umar Sambo, A. U. Ahmad, A. H. Jakada, I. A. Danmaraya, *Quant. Financ. Econ.*, 2021, **5**, 247-263.
[2] E. Billig, M. Decker, W. Benzinger, F. Ketelsen, P. Pfeifer, R. Peters, D. Stolten, D. Thrän, *J. CO2 Util.*, 2019, **30**, 130-141.
[3] E. Lindstad, B. Lagemann, A. Rialland, G. M. Gamlem, A. Valland, *Transp. Res. D Transp. Environ.*, 2021, **101**, article no. 103075.
[4] H. M. Yoo, S. W. Park, Y. C. Seo, K. H. Kim, *J. Environ. Manage.*, 2019, **234**, 1-7.
[5] S. X. Chin, C. H. Chia, S. Zakaria, Z. Fang, S. Ahmad, *J. Taiwan Inst. Chem. Eng.*, 2015, **52**, 85-92.
[6] S. K. Loh, *Energy Convers. Manag.*, 2017, **141**, 285-298.
[7] J. A. Garcia-nunez, D. Tatiana, C. Andr, N. Elizabeth, E. Eduardo, S. Lora, C. Stuart, C. Stockle, J. Amonette, M. Garcia-perez, *Biomass Bioenerg*, 2016, **95**, 310-329.
[8] V. Subramaniam, S. K. Loh, A. A. Aziz, *Sustain. Prod. Consum.*, 2021, **28**, 1552-1564.

[9] F. B. Ahmad, Z. Zhang, W. O. S. Doherty, I. M. O. Hara, *Renew. Sust. Energy Rev.*, 2019, **109**, 386-411.

[10] Y. Krishnan, C. P. C. Bong, N. F. Azman, Z. Zakaria, N. Othman, N. Abdullah, C. S. Ho, C. T. Lee, S. B. Hansen, H. Hara, *J. Clean. Prod.*, 2017, **146**, 94-100.

[11] S. Y. Lee, T. Alam, J. H. Kim, J. C. Lee, S. W. Park, *Biomass Convers. Biorefin.*, 2021, 1-10.

[12] L. J. Hau, R. Shamsuddin, A. K. A. May, A. Saenong, A. M. Lazim, M. Narasimha, A. Low, *Waste Biomass Valorization*, 2020, **11**, 5539-5548.

[13] P. Zhao, Y. Shen, S. Ge, Z. Chen, K. Yoshikawa, *Appl. Energy.*, 2014, **131**, 345-367.

[14] W. H. Chen, B. J. Lin, Y. Y. Lin, Y. S. Chu, A. T. Ubando, P. L. Show, H. C. Ong, J. S. Chang, S. H. Ho, A. B. Culaba, A. Pétrissans, M. Pétrissans, *Prog. Energy Combust. Sci.*, 2021, **82**, article no. 100887.

[15] H. C. Ong, K. L. Yu, W. H. Chen, M. K. Pillejera, X. Bi, K. Q. Tran, A. Pétrissans, M. Pétrissans, *Renew. Sust. Energy Rev.*, 2021, **152**, article no. 111698.

[16] S. S. Qureshi, S. Nizamuddin, H. A. Baloch, M. T. H. Siddiqui, N. M. Mubarak, G. J. Griffin, *Biomass Convers. Biorefin.*, 2019, **9**, 827-841.

[17] P. M. Abdul, J. Jahim, S. Harun, M. Markom, N. A. Lutpi, O. Hassan, V. Balan, B. E. Dale, M. Tusirin, M. Nor, *Bioresour. Technol.*, 2016, **211**, 200-208.

[18] G. Kumar, J. Dharmaraja, S. Arvindnarayan, S. Shoban, *Fuel*, 2019, **251**, 352-367.

[19] H. Hammani, M. El Achaby, K. El Harfi, M. A. El Mhammedi, A. Aboulkas, *C. R. Chim.*, 2016, **15**, 1-12.

[20] A. Agrifoglio, A. Fichera, A. Gagliano, R. Volpe, *C. R. Chim.*, 2016, **15**, 1-12.

[21] R. Y. Chein, W. H. Hsu, *Renew. Energy*, 2020, **153**, 117-129.

[22] Z. Khan, S. Yusup, M. Aslam, A. Inayat, M. Shahbaz, S. Raza Naqvi, R. Farooq, I. Watson, *J. Clean. Prod.*, 2019, **236**, article no. 117636.

[23] B. Li, H. Yang, L. Wei, J. Shao, X. Wang, H. Chen, *Int. J. Hydrog. Energy*, 2017, **42**, 4832-4839.

[24] B. Li, C. Fabrice Magoua Mbeugang, D. Liu, S. Zhang, S. Wang, Q. Wang, Z. Xu, X. Hu, *Int. J. Hydrog. Energy*, 2020, **45**, 26855-26864.

[25] S. A. Salaudeen, B. Acharya, M. Heidari, S. M. Al-Salem, A. Dutta, *Energy Fuels*, 2020, **34**, 4828-4836.

[26] I. Martínez, M. S. Callén, G. Grasa, J. M. López, R. Murillo, *Fuel Process. Technol.*, 2022, **226**, article no. 107074.

[27] A. Inayat, Z. Khan, M. Aslam, M. Shahbaz, M. M. Ahmad, M. I. Abdul Mutalib, S. Yusup, *Int. J. Hydrog. Energy*, 2020, **46**, 30581-30591.

[28] C. F. M. Mbeugang, B. Li, D. Lin, X. Xie, S. Wang, S. Wang, S. Zhang, Y. Huang, D. Liu, Q. Wang, *Energy*, 2021, **228**, article no. 120659.

[29] T. Bunma, P. Kuchonthara, *Process Saf. Environ. Prot.*, 2018, **118**, 188-194.

[30] J. Dong, A. Nzihou, Y. Chi, E. Weiss-Hortala, M. Ni, N. Lyczko, Y. Tang, M. Ducousso, *Waste Biomass Valorization*, 2017, **8**, 2735-2746.

[31] T. Detchusananard, K. Im-orb, F. Maréchal, A. Arpornwichanop, *Energy*, 2020, **207**, article no. 118190.

[32] X. Zhou, X. Yang, J. Li, J. Zhao, C. Li, M. Du, Z. Yu, Y. Fang, *Energy Convers. Manag.*, 2019, **198**, article no. 111899.

[33] X. Zhou, J. Zhao, S. Guo, J. Li, Z. Yu, S. S. Song, J. Li, Y. Fang, *Int. J. Hydrog. Energy*, 2018, **43**, 17091-17099.

[34] K. Kumabe, Y. Hasegawa, H. Moritomi, *ACS Omega*, 2020, **5**, 236-242.

[35] B. Li, H. Yang, L. Wei, J. Shao, X. Wang, H. Chen, *Int. J. Hydrog. Energy*, 2017, **42**, 5840-5848.

[36] M. Shahbaz, S. Yusup, A. Inayat, D. O. Patrick, M. Ammar, A. Pratama, *Energy Fuels*, 2017, **31**, 13824-13833.

[37] S. Pandey, *J. Mol. Liq.*, 2017, **241**, 1091-1113.

[38] X. Chen, L. Wu, F. Liu, P. Luo, X. Zhuang, J. Wu, Z. Zhu, S. Xu, G. Xie, *Environ. Sci. Pollut. Res.*, 2018, **25**, 15980-15989.

[39] S. Barakan, V. Aghazadeh, *Environ. Sci. Pollut. Res.*, 2021, **28**, 2572-2599.

[40] A. Mateus, J. Torres, W. Marimon-Bolivar, L. Pulgarín, *Water Resour. Ind.*, 2021, **26**, article no. 100154.

[41] G. Dou, J. L. Goldfarb, *Fuel*, 2017, **195**, 273-283.

[42] A. M. Elfadly, I. F. Zeid, F. Z. Yehia, M. M. Abouelela, A. M. Rabie, *Fuel Process. Technol.*, 2017, **163**, 1-7.

[43] Y. Kar, *Biomass Bioenergy*, 2018, **119**, 473-479.

[44] B. A. Mohamed, N. Ellis, C. S. Kim, X. Bi, *Renew. Energy*, 2019, **142**, 304-315.

[45] D. D. Sewu, D. S. Lee, H. N. Tran, S. H. Woo, *J. Taiwan Inst. Chem. Eng.*, 2019, **104**, 106-113.

[46] N. Aprianti, M. Faizal, M. Said, S. Nasir, *J. Appl. Eng. Sci.*, 2021, **19**, 334-343.

[47] M. Faizal, N. Aprianti, M. Said, S. Nasir, *J. Appl. Eng. Sci.*, 2021, **19**, 934-941.

[48] S. D. S. Murti, Y. Sudo, S. Yan, Adiarso, R. Noda, *IOP Conf. Ser. Earth Environ. Sci.*, 2018, **105**, article no. 012105.

[49] M. Lasich, *ACS Omega*, 2020, **5**, 11068-11074.

[50] S. Chen, Z. Zhao, A. Soomro, S. Ma, M. Wu, Z. Sun, W. Xiang, *Biomass Bioenergy*, 2020, **138**, article no. 105607.

[51] A. M. Parvez, S. Hafner, M. Hornberger, M. Schmid, G. Scheffknecht, *Renew. Sustain. Energy Rev.*, 2021, **141**, article no. 110756.

[52] S. Hernández, M. A. Farkhondehfal, F. Sastre, M. Makkee, G. Saracco, N. Russo, *Green Chem.*, 2017, **19**, 2326-2346.

[53] K. Jin, D. Ji, Q. Xie, Y. Nie, F. Yu, J. Ji, *Int. J. Hydrog. Energy*, 2019, **44**, 22919-22925.

[54] Y. Lei, R. Zhou, *Util. Environ. Eff.*, 2019, 1-7.

[55] S. Rupesh, C. Muraleedharan, P. Arun, *Resour. Technol.*, 2016, **2**, 94-103.

[56] M. Shahbaz, S. Yusup, A. Inayat, M. Ammar, D. O. Patrick, A. Pratama, S. R. Naqvi, *Energy Fuels*, 2017, **31**, 12350-12357.

[57] R. Tavares, E. Monteiro, F. Tabet, A. Rouboa, *Renew. Energy*, 2020, **146**, 1309-1314.

[58] M. Shahbaz, S. Yusup, A. Inayat, D. O. Patrick, A. Pratama, M. Ammar, *Bioresour. Technol.*, 2017, **241**, 284-295.

[59] Z. Li, Y. Wang, Z. Li, G. Luo, S. Lin, H. Yao, *Fuel*, 2016, **184**, 409-417.

[60] H. Guzman, D. Roldan, A. Sacco, M. Castellino, M. Fontana, N. Russo, S. Hernandez, *Nanomaterials*, 2021, **11**, article no. 3052.

[61] P. Kumari, B. Mohanty, *Int. J. Energy Res.*, 2020, **44**, 6927-6938.

[62] S. A. A. Al-Muraisy, L. A. Soares, S. Chuayboon, S. Bin Ismail, S. Abanades, J. B. van Lier, R. E. F. Lindeboom, *Fuel Process. Technol.*, 2022, **227**, article no. 107118.

[63] C. Li, R. Liu, J. Zheng, Z. Wang, Y. Zhang, *Int. J. Hydrog. Energy*, 2021, **46**, 24956-24964.